

Short Communication

Nonenzymatic Glucose Sensor: Glassy Carbon Electrode Modified with Graphene-Nickel/Nickel Oxide Composite

V. Anitha Kumary^{1,*}, T. E. Mary Nancy¹, J. Divya¹, K. Sreevalsan²

¹Department of Chemistry, Sree Narayana College for Women, Kollam, , Kerala, India 691001

²Department of Chemistry, Sree Narayana College, Kollam, , Kerala, India 691001

* E-mail: anithasreevalsan@gmail.com

Received: 12 December 2012 / Accepted: 11 January 2013 / Published: 1 February 2013

Graphene based sensors receive attention due to their enhanced surface area, unique two – dimensional structure, remarkable stability and excellent electrical conductivity. In the present work graphene-nickel/nickel oxide composite was prepared via solar exfoliation of graphite oxide/nickel acetate precursor. The morphology and structure of the as prepared composite has been characterized by transmission electron microscopy (TEM) & X-ray diffraction (XRD) techniques. The composite was used to modify the glassy carbon electrode surface. Its electrocatalytic activity for the oxidation of glucose in alkaline medium was investigated by cyclic voltammetry. The sensitivity and selectivity of the modified electrode towards glucose oxidation promises its effectiveness as a nonenzymatic glucose sensor for practical applications.

Keywords: Non-enzymatic, Glucose sensor, Graphene, Nickel oxide, Cyclic Voltammetry.

1. INTRODUCTION

Glucose monitoring is an inevitable activity, a diabetic patient should perform in order to postpone or even avoid the progression of microvascular complications like retinopathy, nephropathy, neuropathy and macrovascular complications like stroke and coronary artery disease [1]. There is no other assay performed more frequently than that of glucose because of the enormous increase of diabetic population day by day [2]. Therefore the uprise of highly sensitive and selective, low cost, reliable glucose sensors have been the subject of concern for decades not only in blood sugar monitoring, but also in the food industry, bioprocessing and in the development of renewable, sustainable fuel cells [3-5].

Electrochemical glucose sensors generally fall into two categories viz. enzymatic and non-enzymatic. Though the enzymatic glucose sensors have dominated the market, they suffer various drawbacks that originate from the inherent instability of the enzymes [6]. These difficulties can be

overcome by the use of highly improved, sensitive and selective non enzymatic sensors. Graphene the 2D honey comb lattice of SP^2 bonded carbon atoms, the mother of all graphitic materials attracts researchers by virtue of its unique nano structure and properties. It is the very promising material having excellent electrocatalytic activities. Currently, graphene based nonenzymatic sensors have become a hot area of research due to their enriched surface area, excellent electrical conductivity, cost effectiveness, ease of processing and safety [7]. Graphene is an excellent 2D support to load polymers or nanoparticles. Graphene-metal/metal oxide nanocomposites, with their enhanced properties have marvelously invited strong scientific and technological attention in recent years [8]. Thus graphene based electrode materials have widened the hemisphere of electrochemical glucose sensing by promoting fast electron transfer kinetics [9, 10].

In the present work 2D graphene sheets decorated with 3D Ni/NiO nanoparticles have been synthesized by solar exfoliation [11] of graphite oxide/nickel acetate precursor. The advantages of the present method of synthesis includes: i) It is totally a green chemical route which does not involve any hazardous chemicals.

ii) simultaneous and efficient reduction and exfoliation of metal salt-GO precursors can be achieved. iii) it solves the problem of irreversible agglomeration of graphene sheets, faced by solution based techniques, during drying of the dispersion. iv) it is an economic yet fast process which can be further exploited for the large scale production of graphene and its composites. The dispersed metal/metal oxides act as spacers between the graphene sheets thereby, further protecting its aspect ratio [12]. As nickel is an effective electrocatalyst for glucose oxidation [13], a number of studies on nickel based composites have been conducted [14-22]. In the present work we investigated the electrocatalytic oxidation of glucose in alkaline medium, at solar graphene-Ni/NiO modified glassy carbon electrode. The quick fabrication of the electrode by just drop drying the dispersion of solar graphene-Ni/NiO in methanol is another benefit of this approach. The synergistic effect of graphene and Ni/NiO greatly enhances the performance of the composite in the realm of glucose sensing. This sensor retains good sensitivity and a low detection limit of $0.28\mu\text{M}$.

2. EXPERIMENTAL

2.1. Chemicals

Graphite powder ($< 45\mu\text{m}$), potassium permanganate, nickel acetate and glucose were obtained from Merck. All other chemicals were of analytical grade and used without further purification. High quality deionised water was used throughout

2.2. Preparation of graphite oxide

Graphite oxide (GO) was prepared from graphite powder by an improved Hummer's method [23, 24]. In a typical synthesis 2g of graphite powder was added to a mixture of cold concentrated sulphuric acid (180 ml) and orthophosphoric acid (20 ml). Then 9g of potassium permanganate was

added gradually under stirring, keeping the temperature of the mixture below 20°C. The reaction mixture was then heated to 50°C and kept under magnetic stirring for 12 hours. Then it was cooled and poured into ice containing 4 ml 30% hydrogen peroxide. This mixture was centrifuged and the residue was washed in succession with water, 30% HCl and ethanol. The material obtained after this multiple wash process was coagulated with 100 ml ether and the resulting suspension was filtered, dried and the labeled as GO.

2.3. Preparation of graphene-nickel/nickel oxide composite

The synthesis of graphene-nickel/nickel oxide composite involved two steps. In the first step 60 mg of nickel acetate and 100 mg of GO were dispersed in 200 ml of methanol by sonicating for half an hour. The mixture was then magnetically stirred for 4 hours. The residue was washed well with methanol, centrifuged, dried and labeled as GO-NiAc (graphite oxide-nickel acetate precursor). In the second step, a portion of the GO-NiAc precursor was spread on a petridish and exposed to focused solar radiation using a convex lens of diameter 90mm [11]. The exposure to focused sunlight causes simultaneous exfoliation and reduction of the GO-NiAc composite resulting in a novel material composed of 2D graphene sheets decorated with 3D nickel/nickel oxide nanoparticles. For comparison, solar graphene (sG) and solar nickel/nickel oxide (sNi/NiO) were also prepared separately from GO and nickel acetate respectively.

2.4. Preparation of modified electrodes

Before use, a glassy carbon electrode (GCE, 3.0 mm in diameter) was polished on a polishing cloth with 1.0, 0.3 and 0.05 μ m alumina in succession, each time sonicating twice with methanol and distilled water respectively. 2mg of solar graphene-nickel/nickel oxide composite was dispersed in 1ml methanol by ultrasonication for 2 hours. 5 μ l of the suspension was dropped on the surface of the GCE and dried in air. A solar nickel/nickel oxide electrode was also fabricated similarly for comparison.

2.5. Electrochemical measurements

Cyclic voltammetric studies were conducted using a CHI 604D electrochemical workstation with conventional three electrode cell at room temperature. Modified solar graphene nickel/nickel oxide-glassy carbon electrode or solar nickel/nickel oxide-GCE for comparison, was employed as the working electrode. A silver/silver chloride (Ag/AgCl) electrode acted as the reference electrode and a platinum wire as the counter electrode. The supporting electrolyte was 0.1M sodium hydroxide containing 0.1M potassium chloride. Deionised water was used throughout the experiments.

3. RESULTS AND DISCUSSION

3.1. Characterization of sG-Ni/NiO composite

The as prepared composite was characterized using Transmission electron microscopy (TEM) and X-ray energy dispersive spectroscopy (EDX), on a JEOL 2010F high resolution transmission electron microscope with an accelerating voltage of 200 kV. Figure 1A clearly shows well exfoliated, wrinkled 2D graphene sheets decorated uniformly with nickel/nickel oxide nanoparticles. Figure 1B depicts the EDX spectrum, which shows the presence of only nickel, carbon and oxygen other than copper which comes from the copper grid used for dropping the sample. Powder X-ray diffraction patterns of the as synthesized samples were recorded on Bruker AXS D8 ADVANCE X-ray diffractometer equipped with a $\text{CuK}\alpha$ radiation source ($\lambda = 1.5406 \text{ \AA}$). The XRD patterns as shown in Figure 2 confirm the constitution of the composites.

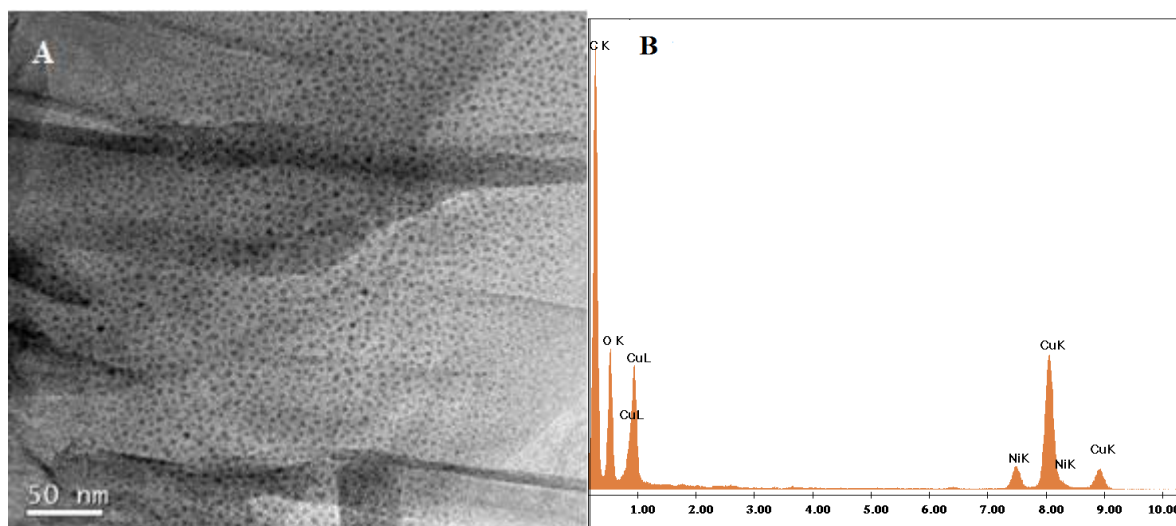


Figure 1. (A) TEM image of sG-Ni/NiO composite, (B) EDX of sG-Ni/NiO composite

The broad peak at 26° can be attributed to the (002) diffraction of solar graphene (sG) [11]. No peak is observed around 10° indicating the successful reduction of GO to sG. Solar nickel/nickel oxide (sNi/NiO) shows eight characteristic diffraction peaks; five at 37.35 , 43.38 , 62.98 , 75.52 and 79.49° , corresponding to the (111), (200), (220), (311) and (222) crystalline planes of nickel oxide (JCPDS card no. 89-7130) and three at 44.58 , 51.93 and 76.44° , corresponding to the (111), (200) and (220) crystalline planes of nickel (JCPDS card no. 87-0712). This reveals that, exposure of nickel acetate to solar radiation for a certain duration, actually converts it into a mixture of nickel and nickel oxide. The close examination of the XRD of solar graphene-nickel/nickel oxide composite (sG-Ni/NiO) shows that it contains, less intense characteristic peaks of nickel and sG in addition to intense characteristic peaks of nickel oxide. The particle size of nickel oxide dispersed in the solar graphene-nickel/nickel oxide composite (sG-Ni/NiO), calculated using the Debye-Scherrer formula based on the full width at half maximum was found to be 168 nm.

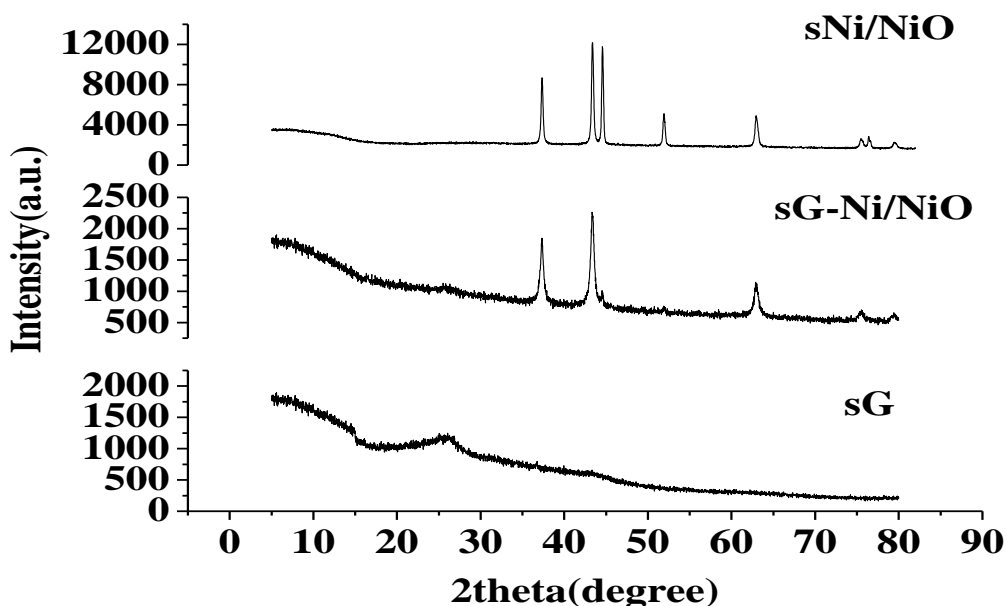
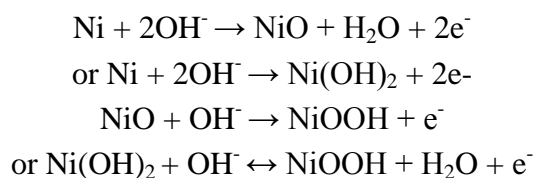


Figure 2. Powder XRD patterns of sG, sG-Ni/NiO composite and sNi/NiO.

3.2. Cyclic voltammograms of modified electrodes

To investigate the electrochemical performance of sG-Ni/NiO modified GCE, cyclic voltammetry (CV) was employed over a potential range from 0.2 to 0.8 V. Figure 3A shows the CVs of sG-Ni/NiO GCE, sNi/NiO GCE and bare GCE in 0.1M NaOH solution, in the absence and presence of 100 μ M glucose at a potential scan rate of 0.05V/s. 0.1M NaOH was chosen as the supporting electrolyte because of two reasons. Firstly an alkaline medium is essential for enhancing the electrocatalytic activity of nickel based materials for oxidation of carbohydrates. Secondly this particular concentration of NaOH gives the best peak current response to glucose [25]. Both sNi/NiO GCE and sG-Ni/NiO GCE do not give obvious redox peaks before further activation, due to the scarcity of Ni(OH)₂ on the electrode surface. After the same electrodes were activated by subjecting them to 10 cycles scan with a CV technique ranging from 0 to 1V, a pair of well defined redox peaks appear with anodic peak around 0.48V and cathodic peak around 0.38V yielding an ΔE_p value of 0.1V. These peaks obtained in the absence of glucose are assigned to the Ni(III)/Ni(II) redox couple. Scanning the electrode up to a high potential results in the conversion of metallic Ni and NiO to Ni(OH)₂ and finally to NiOOH in succession. Thus, enough redox couple is produced, and a pair of redox peaks appears since the hydroxyl groups on the surface of metal oxides are extremely sensitive to electron exposure [21]. The suggested mechanism [26] is as shown below:



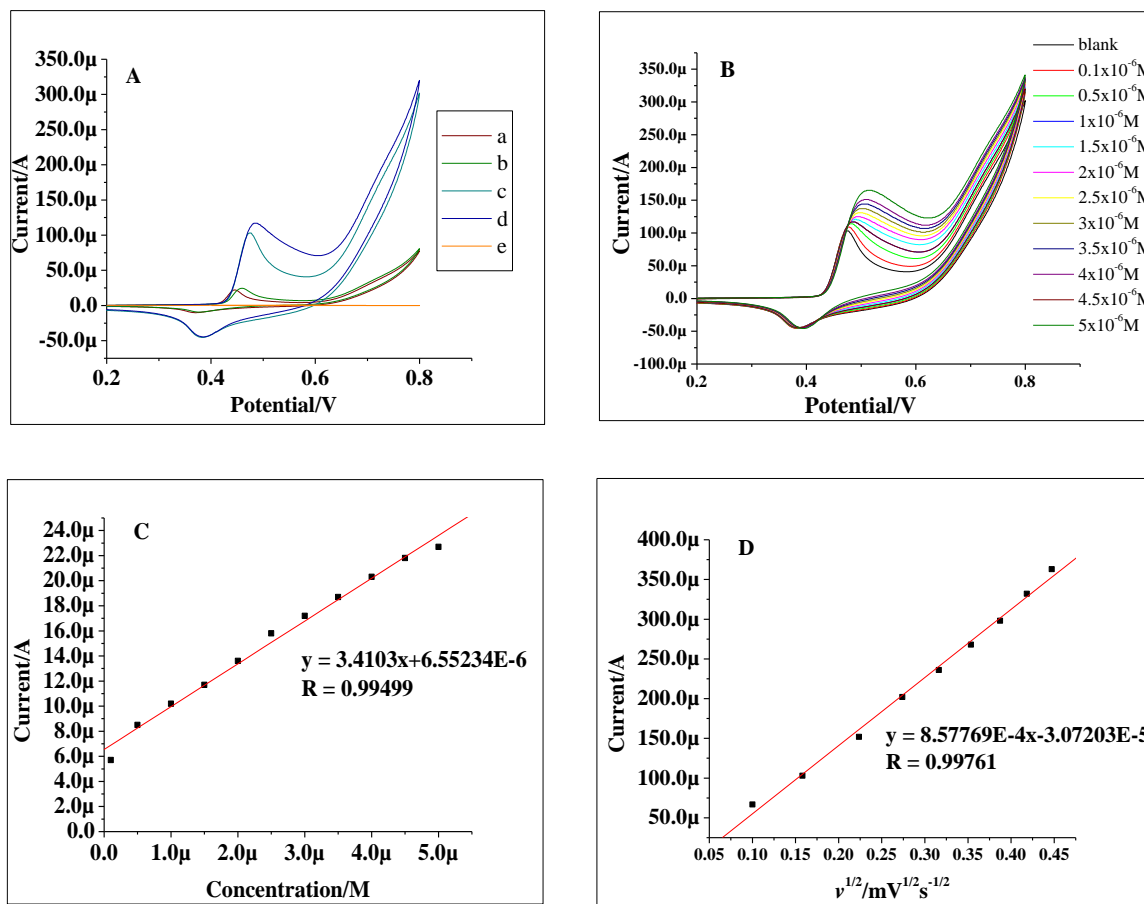


Figure 3. (A) CVs of sG-Ni/NiO GCE (c, d), sNi/NiO GCE (a, b) and bare GCE (e) in the absence and presence of 100µM glucose; (B) CVs of activated sG-Ni/NiO GCE with different glucose concentrations at the scan rate of 50 mV/s; (C) plot of anodic peak current vs. concentration (D) plot of anodic peak current vs. square root of scan rate ($v^{1/2}$).

Figure 3A clearly demonstrates the increase in peak current by 80µA at the sG-Ni/NiO GCE compared to the sNi/NiO GCE. This could be attributed to the presence of more quantity of Ni(OH)₂ in the sG-Ni/NiO composite by virtue of the enhanced surface area attained by the incorporation of graphene, and also to the excellent electroconductibility of graphene promoting fast electron transfer between the Ni/NiO composite and the substrate electrode [25]. Upon addition of 100µM glucose, the anodic peak currents of both the electrodes are enhanced and the cathodic peak currents are decreased. This is due to the change in the Ni(II)/Ni(III) concentration ratio as a result of the rapid electrocatalytic oxidation of glucose, the mechanism for which is as follows [21, 25, 26]:



At the same time bare GCE shows no obvious signal to the NaOH and glucose all the time. Figure 3B depicts the gradual increase in the anodic peak current at the activated sG-Ni/NiO GCE with increasing glucose concentration at the scan rate of 50mV/s. This indicates that the sG-Ni/NiO modified GCE has good sensitivity. The redox reaction occurring at the electrode surface is restricted due to limited

OH⁻ ion diffusion rate which in turn limits diffusion of glucose to the electrode surface as evidenced by a positive shift in peak potentials, showing the diffusion limitation of glucose in the catalytic process [9,21,25]. The oxidative peak currents increased with increase of scan rate and were linearly proportional to the scan rate in the range of 10-200 mV/s (not shown), indicating a surface-controlled electrode process [9]. The oxidation peak current (I_{pa}) also increases linearly with the square root of scan rates ($v^{1/2}$) between 10 and 200 mV/s respectively as shown in Figure 3D. A linear relationship with a correlation coefficient of 0.99761 exists between I_{pa} and $v^{1/2}$. This is a clear indication of a diffusion controlled electrochemical process due to the existence of OH⁻ diffusion transport between the supporting electrolyte and the electrode surface during the reaction process. The redox reaction occurring on the electrode surface [$Ni(OH)_2 + OH^- \leftrightarrow NiOOH + H_2O + e^-$] is restricted due to the limited OH⁻ diffusion rate which in turn limits the following reaction, $NiOOH + \text{glucose} \rightarrow Ni(OH)_2 + \text{glucolactone}$ [10, 21, 25].

The calibration plot (Figure 3C) shows a linear relationship with sensitivity (slope) 3410.3 $\mu\text{A}/\mu\text{M}$ and correlation of 0.99499 over the low concentration range of 0.1-5 μM . To find sensitivity in $\mu\text{A } \mu\text{M}^{-1}\text{cm}^{-2}$, the slope was divided by the area of the electrode [27]. The sG-Ni/NiO sensor exhibits a much higher sensitivity (48,270 $\mu\text{A } \text{mM}^{-1}\text{cm}^{-2}$) compared to other nickel based GCEs reported in literature. Refer Table1. The formula $3\sigma/\text{slope}$ was employed to calculate the detection limit, where σ is the standard deviation of the blank [28]. The detection limit of the electrode by this method is 0.28 μM . The stability and reproducibility of the electrode could be reflected from the fact that there is almost no change in current density on repeating the same tests for more than seven times.

Table 1. Comparison of the analytical parameters obtained at different nickel based GCEs

Sl. No	Modification on GCE	Electrochemical technique employed	Sensitivity	Linear range/ μM	Detection limit/ μM	Reference
1.	sGraphene-Ni/NiO	Cyclic Voltammetry	48,270 $\mu\text{A m M}^{-1}\text{cm}^{-2}$	0.1 - 5	0.28	Present work
2.	RGO-Ni(OH) ₂	Chronoamperometry	11.43 $\mu\text{A m M}^{-1}\text{cm}^{-2}$	2 - 3100	0.6	27
3.	Ni(OH) ₂ -Graphene	Chronoamperometry	494 $\mu\text{A m M}^{-1}\text{cm}^{-2}$ 328 $\mu\text{A m M}^{-1}\text{cm}^{-2}$	1 - 10 10 - 1000	0.6	24
4.	Nickel nanospheres-RGO	Chronoamperometry	813 $\mu\text{A m M}^{-1}\text{cm}^{-2}$ 937 $\mu\text{A m M}^{-1}\text{cm}^{-2}$	1 - 110 1 - 10	-	26
5.	DNA dispersed Graphene-NiO	Chronoamperometry	9 $\mu\text{A m M}^{-1}\text{cm}^{-1}$ 14.3 $\mu\text{A m M}^{-1}\text{cm}^{-1}$	1 - 8000 1 - 200	2.5	10

3.3. Interferences

Ascorbic acid (AA) and Uric acid (UA) are well known common interferents encountered in the detection of glucose [29]. The selectivity of the sensor was evaluated by the CV response of sG-Ni/NiO modified GCE towards glucose (1mM) in presence of UA (0.02mM) and AA (0.1mM) in the physiological level, between 0.2 and 0.8V, at a scan rate of 50mV/s (result not shown). Only a single peak characteristic of 1mM glucose without change in the peak current and potential is obtained. Therefore the as prepared sG-Ni/NiO GCE exhibits good selectivity for glucose detection.

4. CONCLUSIONS

To summarize, sG-Ni/NiO composite has been synthesized successfully by the most green and economic solar exfoliation method. The characterization studies show that the composite is composed of wrinkled graphene sheets on which Ni/NiO nanoparticles are uniformly dispersed. As observed by CV, the sG Ni/NiO modified GC electrode exhibits good sensitivity, stability and selectivity for nonenzymatic glucose detection. The simple preparation procedure, coupled with the low cost and high electrocatalytic activity, unfolds a new pathway for highly economic, reliable, sensitive and selective glucose detection.

ACKNOWLEDGEMENTS

Thanks are due to the UGC for the financial assistance provided.

References

1. J. Wang, *Chem. Rev.*, 108 (2008) 814
2. A. Heller and B. Feldman, *Chem. Rev.*, 108 (2008) 2482
3. M. Vidotti, C. D. Cerri, R. F. Carvalhal, J.C.Dias, R.K.Mendes, S.I.Cordoba de Torresi and L.T.Kubota, *J. Electroanal. Chem.*, 636 (2009) 18
4. M. P. Nandakumar, A. Sapre, A. Lali and B. Mattiasson, *Appl. Microbiol. Biotechnol.*, 52 (1999) 502
5. S. Prilutsky, P. Schechner, E. Bubis, V. Makarov, E. Zussman and Y. Cohen, *Electrochim. Acta*, 55 (2010) 3694
6. E. Reitz, W. Jia, M. Gentile, Y. Wang and Y. Lei, *Electroanalysis*, 20 (2008) 2482
7. Y. Shao, J. Wang, H. Wu, J. Liu, I. A. Aksay and Y. Lin, *Electroanalysis*, 22 (2010) 1027
8. H. Bai, C. Li and G. Shi, *Adv. Mater.*, 23 (2011) 1089
9. W. D. Zhang, J. Chen, L. C. Jiang, Y. X. Yu and J. Q. Zhang, *Microchim. Acta*, 168 (2010) 259
10. W. Lv, F. M. Jin, Q. Guo, Q. H. Yang and F. Kang, *Electrochim. Acta*, 73 (2012) 129
11. S. S. J. Aravind, V. Eswaraiyah and S. Ramaprabhu, *J. Mater. Chem.*, 21 (2011) 17094
12. Y. Si and E. T. Samulski, *Chem. Mater.*, 20 (2008) 6792
13. M. Fleischmann, K. Korinek and D. Pletcher, *J. Electroanal. Chem.*, 31 (1971) 39
14. M. Shamsipur, M. Najafi and M. R. M. Hosseini, *Bioelectrochemistry*, 77 (2010) 120
15. W. Wang, Z. Li, W. Zheng, B. Dong, S. Li, and C. Wang, *J. Nanosci. Nanotechnol.*, 10 (2010) 7537

16. M. S. M. Quintino, H. Winnischofer, M. Nakamura, K. Araki, H. E. Toma and L. Angnes, *Anal. Chim. Acta*, 539 (2005) 215
17. J. Y. Sun, K. J. Huang, Y. Fan, Z. W. Wu and D. D. Li, *Microchim. Acta*, 174 (2011) 289
18. Q. Yi, W. Huang, W. Yu, L. Li and X. Liu, *Electroanalysis*, 20 (2008) 2016
19. C. Li, Y. Liu, L. Li, Z. Du, S. Xu, M. Zhang, X. Yin and T. Wang, *Talanta*, 77 (2008) 455
20. L. M. Lu, L. Zhang, F. L. Qu, H. X. Lu, X. B. Zhang, Z. S. Wu, S. Y. Huan, Q. A. Wang, G. L. Shen and R. Q. Yu, *Biosens. Bioelectron.*, 25 (2009) 218
21. Y. Mu, D. Jia, Y. He, Y. Miao and H. L. Wu, *Biosens. Bioelectron.*, 26 (2011) 2948
22. Y. Zhang, F. Xu, Y. Sun, Y. Shi, Z. Wen and Z. Li, *J. Mater. Chem.*, 21 (2011) 16949
23. W. S. Hummers Jr. and R. E. Offeman, *J. Am. Chem. Soc.*, 80 (1958) 1339
24. D. C. Marcano, D. V. Kosynkin, J. M. Berlin, A. Sinitskii, Z. Sun, A. Slesarev, L.B. Alemany, W. Lu and J. M. Tour, *ACS Nano*, 4 (2010) 4806
25. N. Qiao and J. Zheng, *Microchim. Acta*, 177 (2012) 103
26. C. Zhao, C. Shao, M. Li and K. Jiao, *Talanta*, 71 (2007) 1769
27. Y. T. Shieh, C. M. Wen, R. H. Lin, T. L. Wang, C. H. Yang and Y. K. Twu, *Int. J. Electrochem. Sci.*, 7(2012) 8761
28. B. Ntsendwana, B. B. Mamba, S. Sampath and O. A. Arotiba, *Int. J. Electrochem. Sci.*, 7 (2012) 3501
29. Z. Wang, Y. Hu, W. Yang, M. Zhou and X. Hu, *Sensors*, 12 (2012) 4860